Cosmic Ray Showers and their Relation to the Stratospheric Sudden Warmings

N. A. Kilifarska [1], Y. K. Tassev [2], D. Y. Tomova [3]

[1] Geophysical Institute, Bulgarian Academy of Sciences, Sofia, Bulgaria

[2] Institute for Solar-Terrestrial Influences, Bulgarian Academy of Sciences, Sofia, Bulgaria

[3] Sofia University "St.Kl.Ochridski", Sofia, Bulgaria

e-mail: nkilifarska@geophys.bas.bg

Received: 27 October 2008; Accepted 28 December 2008

Abstract. The purpose of this paper is to analyse the thermo-dynamical response of the stratosphere-troposphere system to the solar corpuscular and electromagnetic forcing during Solar Proton Event in January 2005 (SPE'05). Cross-correlation analysis of the zonal wind and temperature reveals a warming of subtropics and mid-latitudes (with a time delay of about 5 days) and cooling of the polar cap with time lag of 20-30 days. The zonal wind response manifests itself as a strong and almost instantaneous acceleration of the vortex core and delayed westerlies' deceleration at its polar and equatorial edges. The temperature response equatorward of 50^0N are most probably related to the increased solar ultra-violet (UV) radiation, whose effect can not be separated by the cross-correlation technique from those of the corpuscular heating.
Multi-factorial and multivariate statistical analysis of the zonal wind before and after the SPE'05 confirms the leading role of the solar short time variability. Moreover, it turns out that the vertical propagation of planetary waves is strongly influenced by bursts in solar UV and corpuscular radiation. Comparison of the effectiveness of solar and wave forcing shows that solar impact is dominant factor influencing temperature and zonal wind in the period of preparation of final stratospheric warming in 19 March 2005.

Keywords: stratospheric warmings; proton fluxes; waves

Introduction

Living through the light and warm of our star – the Sun, many scientists intuitively feel its important role in almost all processes on the Earth. However, attempts to show undoubtedly its influence on the dynamics of the winter polar stratosphere and troposphere are obscured by the extreme complexity and interdependence of the processes governing the state of the lower atmosphere [1-11]. Unlike most of the investigations trying to establish some relations with 11-year [i.e. 2, 12-17] or 27 days [18-21] variably of the Sun, the aim of this paper is to elucidate effects of short time variably of solar electromagnetic and corpuscular radiation. For this purpose we examined one of the strongest solar proton events - that of January 2005, which is characterized by three consecutive proton flares and coronal mass ejections (CME) on 16, 17 and 21 January. The X7 flare and CME that occurred on January 21 produced the hardest and most energetic proton event of Solar Cycle 23. We have examined the zonal wind and temperature response from the surface up to 10 hPa on the forcing by intense solar proton fluxes measured on board GOES 10 and 11 satellites, bursts in solar electromagnetic radiation as well as internal atmospheric modes like QBO and ENSO, for a period January – March 2005. The purpose was to investigate its effect on the strength of winter polar vortex and its possible relations with major stratospheric warming occurred in 19 March 2005.

Data and method of analysis

Data for atmospheric temperature and zonal wind are taken from NCEP/NCAR (National Centers for Environmental Prediction and the National Center for Atmospheric Research) reanalysis. Eliassen-Palm fluxes (a measure of planetary wave activity) are calculated within the EP5 project CANDIDOS (Chemical and Dynamical Influences on Decadal Ozone Change) - by courtesy of Climate Science Division of Alfred Wegener Institute for Polar and Marine Research.

The intensity of solar proton fluxes is measured on board the geostationary spacecrafts GOES 10 and 11. Measurements from neutron monitors in Climax (42.21N; -85.37W) show the decrease of Galactic Cosmic Rays (GCR) intensity due to the stronger solar wind (known as Forbush effect [22]). As a proxy of solar electromagnetic radiation we used $F_{10.7}$ (solar radio emission on 10.7 cm). Daily values of equatorial zonal wind at 30 hPa are used as a proxy of daily QBO index. Daily values of Southern Oscillation Index (SOI) are taken from Long Paddock website provided by the Queensland Government: (http://www.longpaddock.qld.gov.au/SeasonalClimateOutlook/Southern OscillationIndex/30DaySOIValues/).

The lagged correlation analysis was applied to

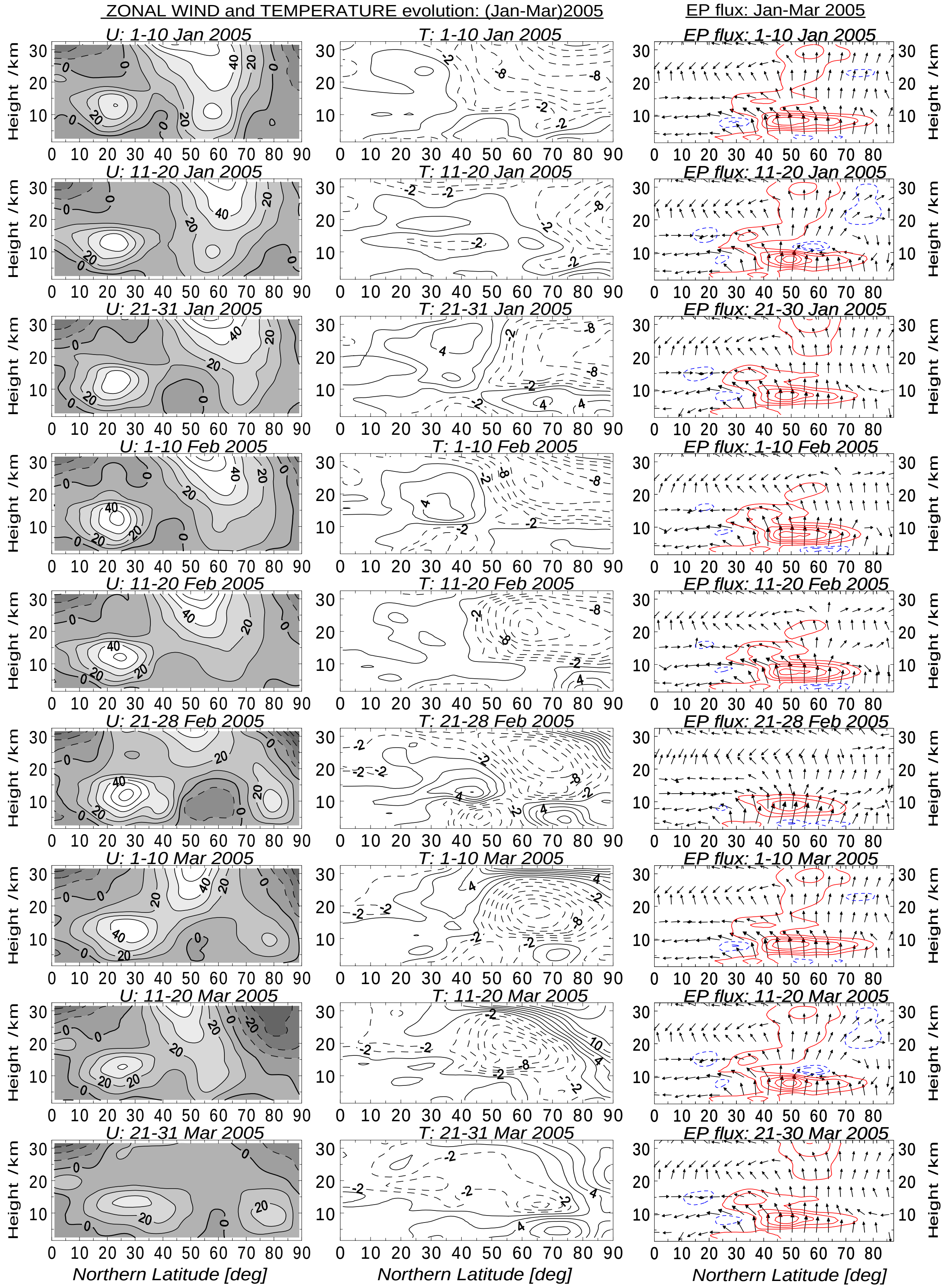

Fig. 1. Time evolution of zonal wind (left column), temperature (middle) and Eliassen-Palm flux (right column) averaged over 10 days. Contours in the right column present Eliassen-Palm flux divergence (continuous lines) and convergence (dashed lines) in units 10^{-5} ms^{-2}.

establish the existence of some time delay in atmospheric response to intense proton fluxes related to Solar Proton Event (SPE). Time series of zonal wind (U), temperature deviations from its 50 years daily mean (dT) and proton fluxes in 7 energetic intervals (E=0.7÷4 MeV, E=4÷9 MeV, E=9÷15 MeV, E=15÷40 MeV, E=40÷80 MeV, E=80÷165 MeV and E=165÷500 MeV) were initially smoothed by 10 points running median procedure.

For closer examination of the time evolution of atmospheric response to changing forcing we stratified each month on 10 day intervals applying multifactorial multivariate regression analysis. Due to strong reduction of the observational points the standard multiple regression analysis becomes inapplicable. For this reason we apply the *Partial Least Square* (PLS) *regression* technique, which generalizes and combines features from principal components analysis and multiple regressions. This approach is particularly useful when we search for relations between a set of dependent variables and a large set of independent variables (i.e. predictors). PLS regression analysis can be used even when the number of observations is small compared to the number of predictors. PLS searches for a set of components (called by some authors: *latent vectors*) that performs a simultaneous decomposition of matrixes of dependent variables **Y** and predictors **X**. The main constrain is that these components must explain as much as possible of the *covariance* between **X** and **Y**. For this aim the independent variables are *decomposed* as $\mathbf{X}=\mathbf{TP}^T$ with $\mathbf{TT}^T=\mathbf{I}$ (identity matrix) and superscript "T" denotes transposed matrix. By analogy of principal component analysis **T** is called the *score* matrix, and **P** the *loading* matrix. Likewise, **Y** is estimated as $\hat{\mathbf{Y}}=\mathbf{TBC}^T$ where **B** is a diagonal matrix with the "regression weights" as diagonal elements. The columns of **T** are the *latent vectors*. To specify **T**, two sets of weights **w** and **c** have to be find in order to create a linear combination of the columns of **X** and **Y** such that their covariance is maximum. Specifically, the goal is to obtain the first pair of vectors $\mathbf{t}=\mathbf{Xw}$ and $\mathbf{u}=\mathbf{Yc}$ with the constraints that $\mathbf{ww}^T=1$, $\mathbf{tt}^T=1$ and $\mathbf{t}^T\mathbf{u}$ be maximal. When the first latent vector (component) is found, it is subtracted from both **X** and **Y** and the procedure is re-iterated until **X** becomes a null matrix.

Synopsis of Northern hemisphere thermodynamics for January - March 2005

Fig.1 presents the time evolution of latitude-altitude distribution of U and dT (temperature anomalies) fields averaged over 10 days. The term "anomaly" used in the text denotes deviation of daily values from corresponding daily averages derived over the 50 years of data available. Fig.1 illustrates quite well the variability of position and strength of polar vortex and temperature anomalies. During and after the SPE (in the middle and end of January) the vortex is moved substantially poleward but from the beginning of February it starts to move back – toward the equator, being shifted by the easterly wind placed over the polar cap. Since the last third of February the temperature over the pole start to increase and at 19 March the criteria of World Meteorological Organisation for major stratospheric warming are fulfilled. At the end of March the stratospheric part of the vortex is completely destroyed and the warming is spread over the mid-latitudes in the troposphere. Examination of the vertical component of Elliasen-Palm (EPz) fluxes – representative of planetary waves vertical propagation (right column in Fig.1), shows that in January the polar vortex serves as a guide for upward propagation of waves, while since February till the middle of March they are severely deflected toward the equator. This means that the planetary waves could hardly be accountable for the formation of easterlies over the pole and the warming starting in the last third of February [11, 23]. For this reason we began a search for some other factors that may be responsible for the observed evolution of polar thermodynamics.

Cross-correlation analysis of proton fluxes intensity and strato-tropospheric profiles of temperature and zonal wind

To detect the time delay between protons forcing and atmospheric response via change of zonal wind and T we provide a lagged correlation analysis for all latitudes between 30^0 and 90^0N at each standard pressure level. Our initial guess was that protons with different energies will have different effect on the atmospheric parameters. So we stratified the whole energy interval on seven intervals (0.7-4; 4-9; 9-15; 15-40; 40-80; 80-165; 165-500 MeV) and calculate cross-correlation coefficients for each of them. A detailed examination of correlation coefficients is very consistent and do not depend significantly on the energy of protons. For this reason we show in Fig. 2 only the correlation coefficients calculated for protons with energies 0.7-4 MeV as a representative for all energy bands.

First that should be noticed in Fig. 2 is a non-uniform response of the atmosphere on proton flux forcing, characterized by warming of mid-latitudes (with maximum near 45^0-50^0N) and cooling - poleward of 55^0-60^0N. The zonal wind oppositely is weakened at mid-latitudes and strengthened at higher latitudes. The maximum enhancement of westerlies is near 60^0N in the stratosphere, however tropospheric zonal wind near 70^0-80^0N is also increased. There is also a narrow area of weak depletion of westerlies placed over the pole (see Fig. 2).

Second important result from the lagged correlation analysis is that T response to the proton forcing is almost instantaneous at subtropics and mid-latitudes (right column, 1st row in Fig.2), while high latitude response is different and more complicated. Thus the decrease of polar troposphere and lower stratospheric T occurs with a delay of 10-30 days, what is consistent with the time scales of downward propagation of NOx species produced by proton fluxes at mesospheric levels [30] and ozone decrease in polar stratosphere. However, due to the reduce amount of sunlight in winter months, the temperature decrease over the polar cap is most probably related to strengthening of the polar vortex, which reduces the mixing with middle latitudes combined with the effect of strong radiative cooling of the atmosphere by Earth's long wave radiation.

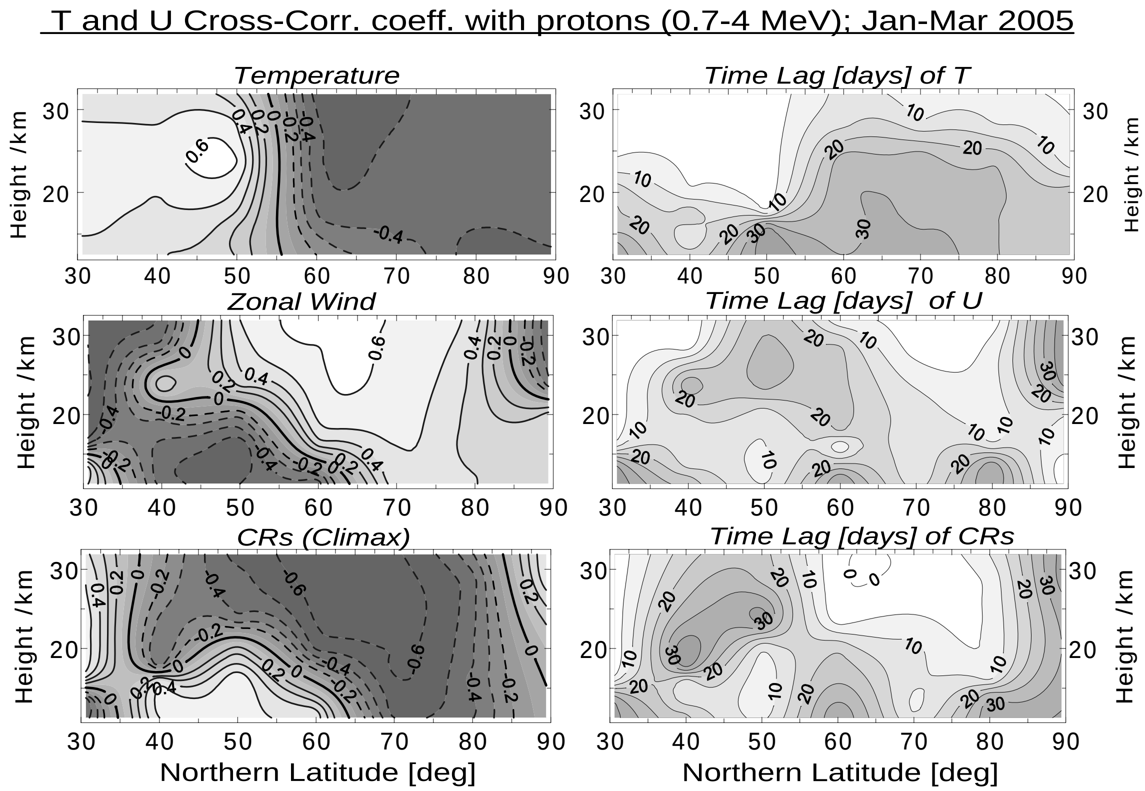

Fig. 2. Cross-correlation coefficients of the temperature (1^{st} row) and zonal wind (middle) with proton fluxes measured on GOES 11. The bottom row presents cross-correlation of the zonal wind and cosmic rays intensity from Climax neutron monitor measurements.

The zonal wind response at 45-65^{0}N latitudes to the solar protons forcing is delayed by 10-25 days, while at 70-75^{0}N the response is almost instantaneous. The delayed response of mid-latitude zonal wind indicates that proton's forcing goes trough the mechanism of atmospheric thermo-dynamical machine, i.e. the warming of mid-latitudes middle stratosphere forces meridional circulation poleward and equatorward from the area of maximum heating transformed by the Coriolis force correspondingly in westerlies and easterlies. More intriguing is almost instantaneous response at high latitudes which hints on a direct exchange of momentum between charged particle in the lower part of their spiral motion around the magnetic field lines and zonal wind.

The bottom row of Fig.2 shows the cross-correlation coefficients and time lag in zonal wind response calculated by the use of neutron monitor measurements in Climax. The obvious similarity with proton fluxes correlations, but with reversed sign, illustrates the Forbush decrease of galactic cosmic rays by solar wind. This means that instead satellite data for proton fluxes intensity we may use Climax neutron monitor counting rates and more precisely their anomalies (i.e. the deviation of daily measurements from the 50 years daily averages), where the sign of anomaly will serve as an indicator of the origin of energetic particles reaching the ground. Thus negative anomalies will indicate intense solar protons while positive one – galactic cosmic rays.

Results from *Partial Least Square* regression of temperature and zonal wind

The results from cross-correlation analysis hint on the existence of relation between intense solar corpuscular radiation and atmospheric winter time variability. However, there is a plenty of works founding evidences of other signals in polar atmosphere like QBO, ENSO, 11-year solar cycle etc. [i.e., 12-17; 24-27, etc.]. For this reason we provide a multivariate PLS regression analysis in attempt to found out the most important combination of factors responsible for occurrence of the major warming in 19 of March. We analyzed separately the impact of: (i) *solar and internal atmospheric variability* and; (ii) *EPz profiles* (as a measure of vertical propagation of planetary waves) on the zonal wind and temperature profiles. Results are presented in Tables 1 and 2 giving the average variance of **zonal wind** and **temperature** described by both groups of forcing factors. We found out that each of the groups is capable to explain between 70% and 90% of total variability of the temperature and zonal wind, depends on the latitude, what shows that strato- troposphere processes are highly interdependent. This makes determination of causality more difficult to realize and it is not surprising that simple correlations between any of the examined forcing factors and atmospheric parameters often become unclear.

The solar influence on the troposphere-stratosphere wave propagating conditions is reported by several authors [i.e., 14, 28 and 29]. In attempt to reveal how much of waves' ability to propagate upward is defined by solar and internal atmospheric modes we made another statistical experiment in which EPz profiles for the period 11-20 March, taken at 50^{0}N latitude, are regressed on: (i) *"current" values* of predictors (i.e.11-20

March); (ii) *lagged by 10 days* predictors' values (i.e., 1-10 March) and; (iii) values of independent variables for *20 days prior the major warming* (i.e., 1–20 March), applying the PLS regression. Results show that in cases of "current" or "old" values of predictors (F10.7, QBO, SOI, Cosmic Rays intensity) regression models can explain up to 70-75% of total variability of planetary waves' vertical propagation (see underlined values in Tables 3 and 4). If 20 days history of predictors is used then up to 99% of EPz variability in the period 11–20 March 2005 is described depending on the number of components included in the regression model (see Table 5).

TABLE 1

Average variance of zonal wind described by solar and internal atmospheric variability (left 5 columns) and by first four components of EPz profile (right 5 columns) for the period 11-20 March 2005

Predictors: F10.7, QBO, SOI, CRs					**Predictors: EPz(height)**				
lat=30^0N					lat=30^0N				
	Increase R2 of Y	**Average R2 of Y**	**Increase R2 of X**	**Average R2 of X**		**Increase R2 of Y**	**Average R2 of Y**	**Increase R2 of X**	**Average R2 of X**
Comp 1	0,652112	0,652112	0,567670	0,567670	**Comp 1**	0,688166	0,688166	0,214107	0,214107
Comp 2	0,145934	0,798046	0,347548	0,915219	**Comp 2**	0,118132	0,806297	0,235767	0,449875
Comp 3	0,049354	0,847400	0,064285	0,979504	**Comp 3**	0,082155	0,888452	0,218291	0,668166
Comp 4	0,031194	**0,878594**	0,020496	1,000000	**Comp 4**	0,013387	**0,901839**	0,136084	0,804250
lat=60^0N					lat=60^0N				
	Increase R2 of Y	**Average R2 of Y**	**Increase R2 of X**	**Average R2 of X**		**Increase R2 of Y**	**Average R2 of Y**	**Increase R2 of X**	**Average R2 of X**
Comp 1	0,447608	0,447608	0,390480	0,390480	**Comp 1**	0,414404	0,414404	0,477679	0,477679
Comp 2	0,146425	0,594033	0,518003	0,908483	**Comp 2**	0,141911	0,556315	0,222427	0,700106
Comp 3	0,206841	0,800875	0,071188	0,979671	**Comp 3**	0,160986	0,717301	0,153050	0,853156
Comp 4	0,009907	**0,810782**	0,020329	1,000000	**Comp 4**	0,086418	**0,803719**	0,126333	0,979489

TABLE 2

Average variance of temperature described by solar and internal atmospheric variability (left 5 columns) and by first four components of EPz profile (right 5 columns) for the period 11-20 March 2005

Predictors: F10.7, QBO, SOI, CRs					**Predictors: EPz(height)**				
lat=30^0N					lat=30^0N				
	Increase R2 of Y	**Average R2 of Y**	**Increase R2 of X**	**Average R2 of X**		**Increase R2 of Y**	**Average R2 of Y**	**Increase R2 of X**	**Average R2 of X**
Comp 1	0,195580	0,195580	0,627161	0,627161	**Comp 1**	0,270110	0,270110	0,316853	0,316853
Comp 2	0,265375	0,460954	0,288732	0,915893	**Comp 2**	0,253268	0,523378	0,239076	0,555929
Comp 3	0,103606	0,564561	0,063560	0,979452	**Comp 3**	0,178536	0,701914	0,146828	0,702757
Comp 4	0,081869	**0,646430**	0,020548	1,000000	**Comp 4**	0,089741	**0,791655**	0,158674	0,861431
lat=60^0N					lat=60^0N				
	Increase R2 of Y	**Average R2 of Y**	**Increase R2 of X**	**Average R2 of X**		**Increase R2 of Y**	**Average R2 of Y**	**Increase R2 of X**	**Average R2 of X**
Comp 1	0,554086	0,554086	0,619593	0,619593	**Comp 1**	0,519541	0,519541	0,619872	0,619872
Comp 2	0,167774	0,721860	0,296717	0,916310	**Comp 2**	0,098417	0,617958	0,259063	0,878935
Comp 3	0,122603	0,844463	0,061535	0,977846	**Comp 3**	0,079481	0,697439	0,083808	0,962743
Comp 4	0,030982	**0,875445**	0,022154	1,000000	**Comp 4**	0,107764	**0,805203**	0,022878	0,985621

TABLE 3

EPz(alt)=f(F10.7,QBO,SOI,CRs)

	Increase $R^2$of Y	**Average $R^2$of Y**	**Increase $R^2$of X**	**Average $R^2$of X**
Comp 1	0,452085	0,452085	0,619315	0,619315
Comp 2	0,107728	0,559813	0,264236	0,883551
Comp 3	0,104642	0,664455	0,095981	0,979531
Comp 4	0,087797	**0,752252**	0,020469	1,000000

TABLE 4

EPz(alt)=f(lagged F10.7, lagged QBO, lagged SOI, lagged CRs)

	Increase $R^2$of Y	**Average $R^2$of Y**	**Increase $R^2$of X**	**Average $R^2$of X**
Comp 1	0,477491	0,477491	0,698201	0,698201
Comp 2	0,175511	0,653002	0,205378	0,903578
Comp 3	0,024057	0,677059	0,072609	0,976188

Waves' or solar forcing?

Going back to Fig. 1 we try to understand why during the whole January the planetary wave propagates freely upward and what an obstacle for wave propagation appears since the beginning of February.

To answer this question we arranged multivariate PLS regression of zonal wind profiles for three distinct episodes of wave propagation evolution: 21-28 February, 1-10 March and 11-20 March using 20 day history of $F_{10.7}$, QBO, and CRs intensity for each of the examined periods. Specifically, EPz profiles for 21-28 February period is regressed on the predictors values taken for the period 10-28 February; EPz profiles from 1-10 March are regressed on the 21 February-10 March of predictors and so on. The calculated 2D regression coefficients are shown in Fig. 3.

One can see that continuously increasing ability of waves to penetrate the middle stratosphere since the last third of February till the occurrence of stratospheric warming in 19 March due to the improvement of wave propagation conditions. Thus if in the end of February all of examined factors anti-correlate with EPz (see 1st column of Fig.3), in the beginning of March correlation coefficients of $F_{10.7}$ and QBO above 15 km become F10.7 and QBO favour wave propagation above the polar cap, while cosmic rays ensure a channel for upward propagation of the waves near 55^0N latitude. A glance on the time series of $F_{10.7}$ and CRs for this period (see Fig.4) shows an increase of both solar electromagnetic and corpuscular radiation just before the stratospheric warming event.

The multivariate PLS regression of *zonal wind* during 11-20 March on the 20 day history of $F_{10.7}$, QBO and cosmic rays intensity from Climax, shows (Fig.5) that short

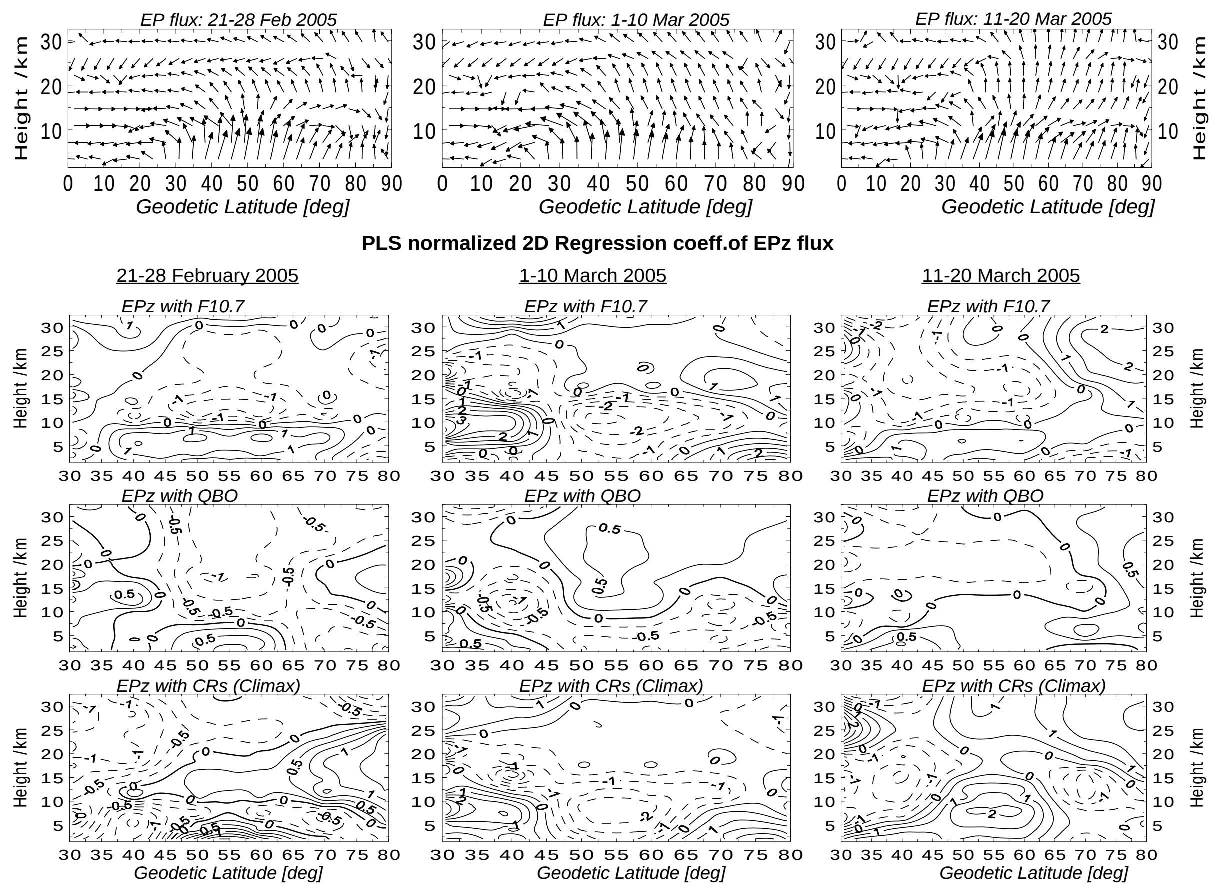

Fig.3. First row: EP fluxes for 3 distinctive periods of planetary waves propagation: 21-28 February, 1-10 and 11-20 March. In the last period a major stratospheric warming occurred. Bottom 3 rows: PLS 2D regression coefficients of EPz flux with $F_{10.7}$, QBO and CRs intensity.

TABLE 5

EPz(alt)=f(F10.7,QBO,SOI,CRs,lagged F10.7, lagged QBO, lagged SOI, lagged CRs)

	Increase $R^2$of Y	Average $R^2$of Y	Increase $R^2$of X	Average $R^2$of X
Comp 1	0,498441	0,498441	0,601276	0,601276
Comp 2	0,236448	0,734889	0,133420	0,734696
Comp 3	0,074240	0,809130	0,163499	0,898195
Comp 4	0,083402	*0,892532*	0,059676	0,957872
Comp 5	0,043910	0,936442	0,028589	0,986460
Comp 6	0,029393	0,965835	0,007708	0,994169
Comp 7	0,013790	0,979625	0,005719	0,999888
Comp 8	0,010744	**0,990369**	0,000112	1,000000

slightly positive. In the weak just before the warming - time variability of solar electromagnetic and corpuscular radiation in a consistent way "work" to reduce the westerlies on the polar edge of the vortex and increase them on its equatorial side. The impact of QBO in these processes is a bit smaller.

Conclusions

A detailed analysis of the evolution of Northern Hemisphere polar vortex after the solar proton event in January 2005 reveals the leading role of short-time variability of solar electromagnetic and corpuscular radiation in thermo-dynamical forcing of the winter time polar stratosphere-troposphere system. The lag correlation analysis of temperature and zonal wind response to the solar protons' forcing shows warming of middle atmosphere southward of 55^0N, appearing almost immediately after the penetration of intense proton fluxes in the atmosphere.

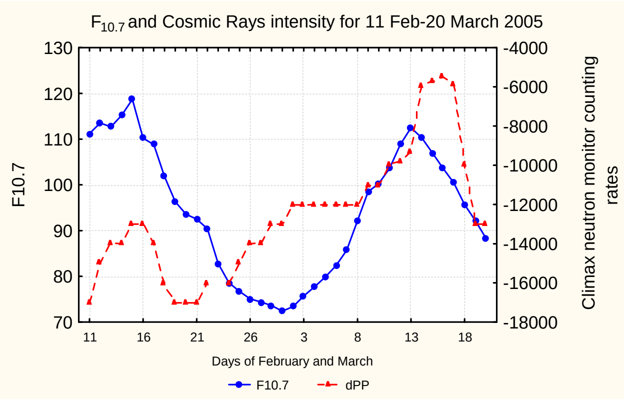

Fig. 4. Time series of $F_{10.7}$ and counting rates of Climax neutron monitor for the period 11 February-20 March 2005.

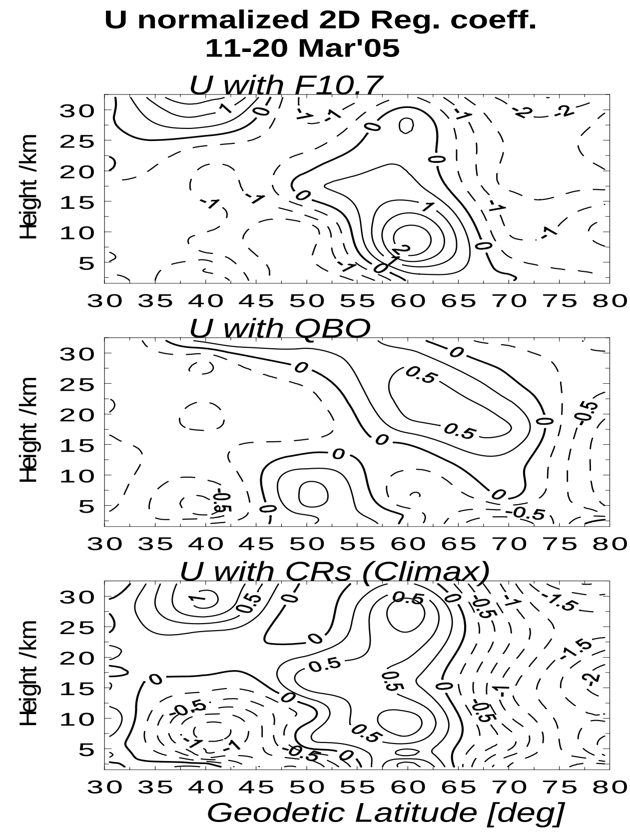

Fig. 5. Multivariate normalized 2D PLS regression coefficients of zonal wind profiles at latitudes 30-80^{0}N.

At mid latitudes, the zonal wind response occurs with some delay, what hints on the mechanism of influence – most probably through low effective atmospheric thermo-dynamical machine. The more curious is almost immediate response of zonal winds at high latitudes (northward of 70^{0}N) and we hypothesize that it may be related to a direct exchange of momentum between highly energetic particles and zonal wind.

Multivariate statistical analysis of the influence of internal atmospheric modes (QBO and ENSO), solar short time variability and EPz fluxes (as a measure of vertical propagation of planetary waves) on atmospheric thermodynamics show that the accuracy of statistical models based separately on: (i) solar and atmospheric variability and (ii) EPz vertical profiles, is comparable and vary between 70% and 90% of total atmospheric variability (depending on latitude) described by each of the models. This interdependence of the factors affecting atmospheric thermo-dynamical regime arise an important question – how much of waves' vertical propagation variability is explained by the forcing from solar and internal atmospheric modes? At 50^{0}N latitude and for the period of occurrence of major warming (11-20 March) the answer is up to 99% of total variability of EPz flux profile, depending on the number of components (*latent vectors*) included in the model. This result shows that solar forcing not only affects the atmospheric thermodynamics but alters as well wave propagation conditions.

Partial least square regression of U profiles show also that the burst of solar UV and corpuscular radiation - just before the stratospheric warming event (19 March 2005) - weakens the polar edge of the vortex and strengthens its equatorial side. This obviously is the main reason for displacement of the polar vortex from the pole followed by the stratospheric warming.

Acknowledgments

This research is partially supported by NSF of Bulgaria, contract No. 1518/05. The authors thanks the Climate Science Division of Alfred Wegener Institute for Polar and Marine Research and specially team of EP5 project CANDIDOS for providing calculation of EP flux. We also acknowledge NCEP/NCAR reanalysis project team for making their data available.

REFERENCES

[1] A.J.Charlton, L.M. Polvani, "A New Look at Stratospheric Sudden Warmings. Part II: Evaluation of numerical models simulations", J. Climate, 2007, v. 20, pp. 470-488.

[2] D.Rind, J.Lean, J.Lerner, P.Lonergan, A.Leboissitier, "Exploring the Stratospheric-Tropospheric Response to Solar Forcing", J. Geophys. Res., 2008, v. 113, D24113, doi: 10.1029/2008JD010114.

[3] A.J.Charlton, L.M. Polvani, "A New Look at Stratospheric Sudden Warmings. Part I: Climatology and modelling benchmarks", J. Climate, 2007, v. 20, pp. 449-469.

[4] R.K.Scott, L.M.Polavani, "Internal Variability of Winter Stratosphere. Part I: Time independent forcing", J. Atmos. Sci., 2006, v. 63, pp. 2758-2776.

[5] R.K.Scott, L.M.Polavani, "Internal Variability of Winter Stratosphere. Part II: Time-dependent forcing", J. Atmos. Sci., 2008, v. 65, pp. 2375-2388, doi:10.1175/2007JAS2619.1

[6] L.Limpasuvan, D.Thompson, D.Hartman, "On the Life Cycle of the Northern Hemisphere Sudden Stratospheric Warmings", J. Climate, 2004, v. 17, pp. 2584-2596.

[7] N.Harnik, R.Lindzen, "The Effects of Reflecting Surfaces on the Vertical Structure and Variability of Stratospheric Planetary Waves", J. Atmos. Sci., 2001, v. 58, pp. 2872-2894.

[8] Y.Kuroda, K.Kodera, "Variability of the Polar Night Jet in the Northern and Southern Hemispheres", J. Geophys. Res., 2001, v. 106, n. D18, pp. 20703-20713.

[9] M.Balduin, J.Holton, "Climatology of Polar Vortex and Planetary Wave Breaking", J. Atmos. Sci., 1988, v. 45, pp. 1123-1142.

[10] M.McIntare, "How Well do We Understand the Dynamics of the Stratospheric Warmings?", J. Meteor. Soc. Japan, 1982, v. 60, pp. 37-52.
[11] K.Kodera, "Solar Influence on the Special Structure of NAO During Winter", J. Geophys. Lett., 2003, v. 30, 1175, doi:10.1029/2002GL016584.
[12] A.Ruzmaikin, J.Feynman, "Solar Influence on a Major Mode of Atmospheric Variability", J. Geophys. Res., 2002, v. 107, n. D14, 4209, doi:10.1029/2001JD001239.
[13] N.F.Arnold, T.R.Robinson, "Solar Cycle Changes to Planetary Wave Propagation and Their Influence on the Middle Atmosphere Circulation", Ann. Geophysicae, 1998, v. 16, pp. 69-76.
[14] C.D.Camp, K.KTung, "The Influence of Solar Cycle and QBO on the Late Winter Stratospheric Polar Vortex", J. Atmos. Sci., 2007, v. 64, n. 4, pp. 1267-1283.
[15] L.Gray, S.Crooks, C.Pascoe, S.Sparrow, M.Palmer, "Solar and QBO Influence on the Timing of Stratospheric Sudden Warmings", J. Atmos. Sci., 2004, v. 61, n. 23, p. 2777-2796.
[16] G.R.Sonnemann, M.Grygalashvyly, "The Relationship Between the Occurrence Rate of Major Stratospheric Warmings and Solar Lyman-Alpha flux", J. Geophys., Res., 2007, v. 112, D20101, doi:10.1029/2007JD008718.
[17] L.L.Hood, "The Temporal Behaviour of Upper Stratospheric Ozone at Low Latitudes: Evidence from Nimbus 4 BUV Data for Short-Term Responses to Solar Ultraviolet Variability", J. Geophys. Res., 1984, v. 89, n. D6, pp. 9557-9568.
[18] L.L.Hood, S.Zou, "Stratospheric Effects of 27-day Solar Ultraviolet Variations: An Analysis of UARS MLS Ozone and Temperature Data", J. Geophys. Res., 1998, v. 103, n. D3, pp. 3629-3638.
[19] L.Chen, J.London, G.Brasseur, "Middle Atmospheric Ozone and Temperature Responses to Solar Irradiance Variations Over 27-day Periods", J. Geophys. Res., 1997, v. 102, n. D25, pp. 29957-29979.
[20] V.Williams, J.Austin, J.D.Haigh, "Model Simulations of the Impact of the 27-day Solar Rotation Period on Stratospheric Ozone and Temperature", Adv. Space Res., 2001, v. 27, n. 12, pp. 1933-1942.
[21] P.I.Y.Velinov, G.Nestorov, L.I.Dorman, "Cosmic Rays Effects on the Ionosphere and on the Radiowaves Propagation", Publishing House of the Bulgarian Academy of Sciences, Sofia, 1974, 312 pages.
[22] M.E.McIntare, T.N.Palmer, "Breaking Planetary Waves in the Stratosphere", Nature, 1983, v. 305, pp. 593-600.
[23] Y.Naito, I.Hirota, "Interannual Variabilityof the Northern Winter Stratospheric Circulation Related to the QBO and the Solar Cycle", J. Meteor. Soc. Jpn., 1997, v. 75, pp. 925-937.
[24] K.Labitzke, H. Van Loon, "Association Between the 11-year Solar Cycle, the QBO and the Atmosphere", J. Atmos. Terr. Phys., 1988, v. 50, n. 3, pp. 197-206.
[25] M.Salby, P.Callaghan, "Connection between the Solar Cycle and the QBO: The Missing link" J. Climate, 2000, v. 13, pp. 2652-2662.
[26] V.Bucha, V.Bucha Jr., "Geomagnetic Forcing of Changes in Climate and in the Atmospheric Circulation", J. Atmos. Terr. Phys., 1998, v. 60, n. 1, pp. 145-169.
[27] K.Kodera, Y.Kuroda, "Dynamical Response to Solar Cycle", J. Geophys. Res., 2002, v. 107, n. D24, 4749, doi:10.1029/2002JD002224.
[28] N.Balachandran, D.Rind, "Modelling the Effects of UV Variability and the QBO on the Troposphere-Stratosphere System. Part. I: The Middle Atmosphere", J. Climate, 1995, v. 8, pp. 2058-2079.
[29] D.Rind, N.Balachandran, "Modelling the Effects of UV Variability and the QBO on the Troposphere-Stratosphere System. Part. II: The troposphere", J. Climate, 1995, v. 8, pp. 2080-2095.
[30] C.H.Jackman, D.Marsh, F.Vitt, R.R.Garcia, E.L.Fleming, G.J. Labow, C.E.Randall, M.L´opez-Puertas, B.Funke, "Short- and Medium-Term Atmospheric Effects of Very Large Solar Proton Events", Atmos. Chem. Phys. Discuss., 2007, v. 7, pp. 10543–10588.